Multidiszciplináris Tudományok, 15. kötet, 2. sz. (2025) pp. 137–144. ***https://doi.org/10.35925/j.multi.2025.2.9***

TREATING C45 STEEL WITH SOLID POWDER ALUMINIZING FOR SELECTIVE SOLDERING TOOL APPLICATIONS

Shohruh Rakhmataliev
PhD student, University of Miskolc, Institute of Physical Metallurgy, Metalforming and Nanotechnology
3515 Miskolc-Egyetemváros, e-mail: shohrux2596@gmail.com

Zsolt Sályi
research fellow, University of Miskolc, Institute of Physical Metallurgy, Metalforming and Nanotechnology
3515 Miskolc-Egyetemváros, e-mail: zsolt.salyi@uni-miskolc.hu

Márton Benke
research fellow, University of Miskolc, Institute of Physical Metallurgy, Metalforming and Nanotechnology
3515 Miskolc-Egyetemváros, e-mail: marton.benke@uni-miskolc.hu

Abstract

Steel (and metals, in general) substrates exhibit good wettability with metal melts due to the similar bonds. However, when immersed in the melt, dissolution of substrate atoms usually occurs, which leads to the degradation of substrate. To enhance the dissolution resistance of the substrate, ceramic coatings are applied as barriers in such applications, where good wetting is not a requirement. When good wettability must be maintained (for instance, soldering nozzles), the enhancement of dissolution resistance is not that easy. The aim of our research is to test novel surface modification methods of steel substrates to enhance the dissolution resistance against metal melts whilst maintaining good wettability. Based on its favourable properties, solid powder aluminizing was chosen as the applied treatment. The present manuscript presents the establishment of the aluminizing set-up, the treatment parameters and the first obtained aluminized steel samples.

Keywords: *powder pack aluminizing, soldering tool, dissolution resistance*

1. Introduction

Nowadays, the transition from conventional Sn–Pb solders to lead-free alternatives has become essential due to environmental regulations and reliability requirements in electronic packaging. Among various lead-free solder systems such as Sn–Ag, Sn–Cu, Sn–Zn, and Sn–Bi, Sn–Ag–Cu (SAC) alloys are widely recognized as the most promising materials because of their favorable melting behavior, good wettability, and superior mechanical properties (Kim et al., 2003; Wu et al., 2004). As a result, SAC solders have been extensively applied in ball-grid-array (BGA) and ceramic BGA interconnections in the form of solder balls and pastes (Farooq et al., 2001). The reliability of SAC solder joints is strongly governed by interfacial reactions and the formation of intermetallic compounds (IMCs) during soldering and service. Previous studies have shown that IMC morphology and growth behavior at Sn–Ag–Cu/Cu and Sn–Ag–Cu/Ni interfaces significantly influence joint

strength and long-term reliability (Yoon et al., 2005; Yu and Wang, 2008). In particular, excessive IMC growth and surface roughening at the solder/substrate interface may degrade mechanical performance under thermal and mechanical loading conditions (Kim et al., 2003). In addition to joint reliability, molten Sn-based solders are known to aggressively react with iron-based soldering tools. At typical soldering temperatures (~593 K), FeSn and $FeSn_2$ intermetallic phases readily form at the Fe/Sn interface, leading to material degradation and tool failure (Kondo, 2015; Heinzel et al., 2017). Although surface modification techniques such as Ni coating are often employed to suppress iron dissolution, nickel itself reacts with molten tin to form Ni–Sn intermetallic compounds, limiting the long-term effectiveness of this approach (Yoon et al., 2005; Kang et al., 2006). Also, Hiroshi Nishikawa et al. examined the relationship between addition of Sn-Ag solder with additional Co and with metals such as clad iron and Cu were studied to determine the effect of adding Co to Sn-Ag solder on the dissolution of the clad iron and the formation of intermetallic compound. The addition of Co to Sn-3.5Ag solder is very effective in reducing the melting thickness of coated iron and the effect of Co addition to Sn-3.5Ag solder on the wetting of Sn-3.5Ag solder on Cu did not except that when reflowing the Co-added solder, the IMC thickness increased significantly regardless of the Co content compared to the binary Sn-3.5Ag solder (Nishikawa et al., 2005). J. Watanabe et al. to prevent the erosion of the soldering iron tip, focused on the use of multi-walled carbon nanotube (MWCNT) composite coating with high strength and high thermal conductivity. From the results of the erosion resistance test, it was shown that the Fe-graphite and Fe-MWCNT composite coating layers have the effect of reducing erosion in molten SAC305 compared to the Fe coating layer (Watanabe et al., 2019). M. Benke et al. undertook an extensive examination to elucidate the interaction dynamics between TiB_2-coated steel specimens and a Sn-Ag-Cu-based solder solution. The 40-day static immersion test between oxide layer-free TiB_2 and the Sn-Ag-Cu solder solution also revealed an absence of new phase formation, dissolution of Sn, Fe, and Ti atoms, or any reaction between TiB_2 and the solder melt (Benke et al., 2019). Zsolt Salyi et al. conducted a comprehensive investigation to assess the effectiveness of a two-phase (FeB / Fe_2B) iron boride coating applied to diverse steel substrates (DC04, C45, CK60, and C105U) in relation to their interaction with the SAC309 lead-free solder liquid alloy, commonly employed in soldering equipment. The experimental findings revealed pronounced resistance to corrosion on the original steel surfaces at the interfaces with the SAC alloy. After 40 days of continuous immersion in SAC309 solder solution, a reduction in the thickness of the boride layers was unchanged across all examined steel substrates. Importantly, the morphology of the layers remained unchanged, providing assurance of stability under prolonged exposure to the solder alloy (Salyi et al., 2022).

Conventional solid powder aluminizing, utilizing a stationary diffusing box, necessitates aluminizing temperatures to reach 900–1,000 °C, resulting in elevated energy consumption and diminished efficiency. This high-temperature processing induces coarse microstructures, distortion, and performance degradation in the workpiece. The significance of the aluminization process extends to the production of steel sheets employed across various industries, including electrical appliances and automotive manufacturing. These sheets play a crucial role in fabricating components designed for high-temperature applications such as ovens, mufflers, and exhaust pipes. However, challenges emerge as aluminized sheets may manifest vulnerability to corrosion, particularly in specific regions such as seams or adhesives, and may exhibit uncoated points, thereby posing potential risks of future material damage (Bayer, 1995; Bates, 2009). Aluminized steels have not been tested against lead-free solder melts so far. Thus, the objective of the present research is to examine the behaviour of aluminized steels substrates

in molten lead-free solder melts. This manuscript reports the production of solid powder aluminizing equipment and the first solid powder aluminizing experiment.

2. Experimental

For the experiments, the fabrication of a reaction container was required. The volumetric capacity of the designed container was determined to be 1000 cm³ to be able to contain multiple specimens of the size of ~4 mm × 12 mm × 16 mm. The container was prepared from SINOXX 4841 type heat resistant steel. The composition of (the Austenitic heat-resisting steel X15CrNiSi25-21) type heat resistant steel is given in *Table 1*.

Table 1

The composition of the heat resistant steel

C	Si	Mn	Ni	P	S	Cr	N
max 0.2	1.5–2.5	max 2	19–22	max 0.045	max 0.015	24–26	max 0.11

Besides the two lids, a top cover is also needed to encapsulate the reaction container. All parts of the reaction bow are shown in *Figure 1*. Remarkably, this container demonstrates a robust heat resistance, capable of withstanding temperatures of up to 2000 °C.

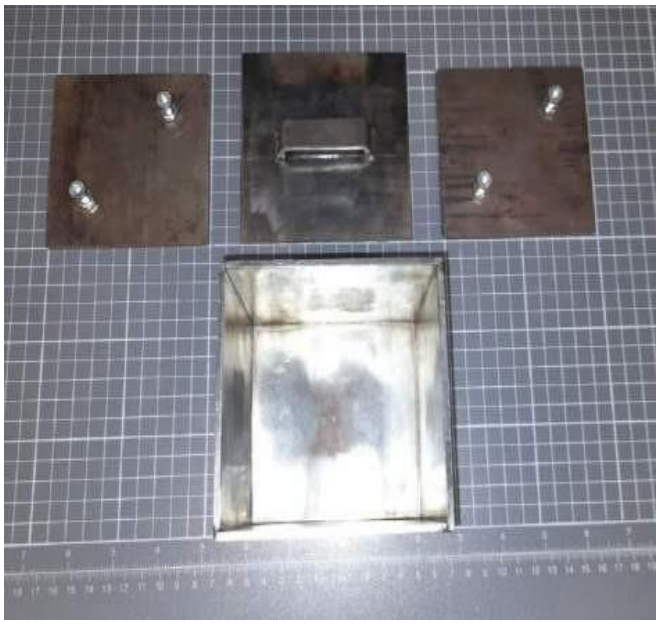

Figure 1. *All parts of the reaction container*

Prior to powder aluminizing experiments, it was essential to assess the container's heat resistance. To do so, the empty reaction container was heated up to the temperature of 1000 °C in a muffle furnace for a duration of 25 minutes. After a duration of 25 minutes, the container was removed from the furnace

and it was observed that the condition, shape and dimensions of the container remained unaltered. Notably, there was no evidence of melting observed either within the container or on the surface of the lids, as depicted in *Figure 2*.

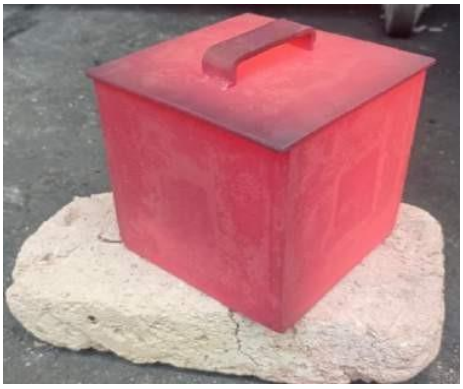

Figure 2. *The container after it has been removed from the furnace*

For the whole research, C45 type steel was selected as base material, being cheap and easily obtainable. The composition of the C45 type steel is given in *Table 2*. Brick-shaped substrate specimens with dimensions of ~ 4 mm × 12 mm × 16 mm were machined from blocks of C45 steel.

Table 2

The nominal m/m% composition of C45 type steel (Yao Teng Steel Brand)

C	S	Mn	P	Si
0.43-0.50	0.60-0.90	0.04	0.050	0.38

Prior to commencing the first powder aluminizing experiment, the surfaces of the steel substrates were meticulously cleaned using alcohol to eliminate any traces of grease and dust. Subsequently, the requisite materials for our aluminizing experiments were prepared. Initially, the FeAl powder (purchased from Metal Powder Company Limited (MEPCO)), was weighed, followed by the addition of ammonium chloride (NH_4Cl, purchased from PGChem company (PGChem company)), to facilitate the dissolution of FeAl. The quantities of these materials utilized are as follows. FeAl was selected to be of 99.5 m/m%, with the remaining 0.5 m/m% comprising NH_4Cl. We measured out 356.644 g of FeAl powder and determined the total mass required by considering it as 99.5% of the mixture. Accordingly, the amount of NH_4Cl required was calculated to be 1.786 g, resulting in a total required mass of 358.43 g. Subsequently, we meticulously blended the FeAl powder and NH_4Cl powder together to obtain a homogenous mixture. Once the mixture was prepared, it was carefully poured into the reaction container. After a uniform layer of the mixture was formed, the C45 steel substrates were positioned within the container, and they were covered with the FeAl and NH_4Cl powder mixture. When NH_4Cl decomposes at high temperatures, $AlCl_3$ passes into a gaseous state, which activates the diffusion of Al atoms to the metal surface. As a result, Fe–Al intermetallic phases are formed on the surface of C45 steel. To improve the quality of the aluminization process and limit the ingress of oxygen into the reaction zone, two protective layers were used. The layers used in the experiment perform specific

physicochemical functions. The Al_2O_3 (Alumina) layer serves to evenly distribute heat and limit the penetration of oxygen into the reaction zone. Al_2O_3 is an inert and highly heat-resistant material that helps stabilize the reaction environment. The SiC (Silicon Carbide) layer is the main outer protective layer that blocks the diffusion of air or oxygen from above. SiC is characterized by very high heat resistance and low gas permeability. This layer isolates the reaction medium from the external atmosphere, ensuring clean, stable, and controlled operation of the internal layers. The powder mixture with the steel substrates in it (the reaction region) was shielded with a steel lid.

This arrangement of the layers is necessary to reduce the risk of uncontrolled oxidation by oxygen during the experimental process, to create stable diffusion conditions, and to form an optimal aluminide layer. *Figure 3* illustrates the schematic representation of the whole set-up of the reaction container ready for the powder aluminizing experiment. These layers were placed one on top of the other, each layer was covered with a separate steel lid, and the entire system was isolated as a reaction medium. Additionally, a lower layer is formed, identified as the Ferro Aluminium layer (FeAl), which serves to encapsulate the surface of the C45 steel substrate.

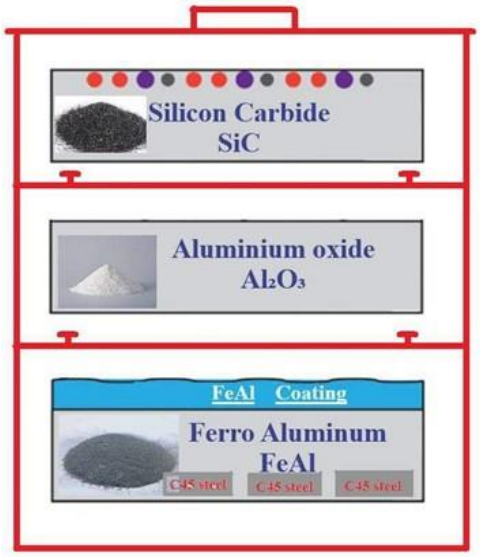

Figure 3. *Provides a schematic overview of the aluminization system, clearly showing the sequence of layers and their functions*

The prepared container was placed in a muffle furnace and held at 1050 °C for 6 hours. During this process, NH_4Cl evaporates and temporarily forms $AlCl_3$. This allows Al atoms to migrate from FeAl to the steel surface. As a result, at high temperatures, Al atoms diffuse into the steel and a protective aluminide layer is formed. This process is based on the "pack aluminizing" mechanism. The aluminized specimens were embedde, than mechanically polished, then etched in 2% Nital for optical microscope examinations. A Zeiss Axio Imager M1m equipped woith motorized sample stage device was used for the optical microscope investigations.

3. Results

The optical microscope mosaic image of an aluminized C45 steel specimen reveals the uniform,

continuous coating along the surface of the steel specimen. This observation proves the interaction between the FeAl powder and the C45 steel, resulting in the deposition or diffusion of Al into the steel surface regions. This observation is corroborated by the affirmative outcome depicted in *Figure 4*.

Figure 5 shows images of the coating formed on the surface of the C45 steel substrate. In *Figure 5* a, the substrate is still visible, while in *Figure 5b*, the coating can be seen with larger magnification. It is apparent, that no cracks were detected within the coating. This observation indicates a uniform distribution of aluminum across the surface of the C45 steel.

Figure 4. *Mosaic optical microscope image of an aluminized C45 steel specimen*

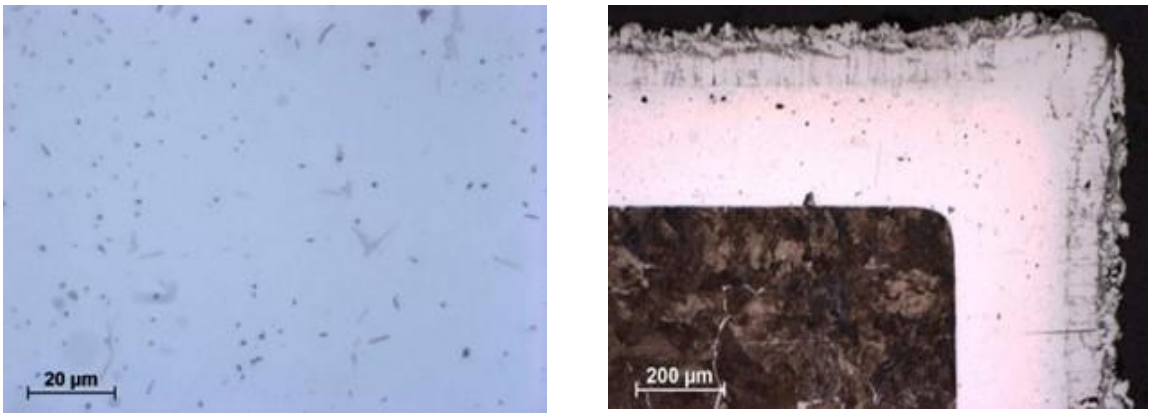

a) b)

Figure 5. *Images of the coating formed on the surface of the C45 steel substrate*

4. Summary

In the present research, the experimental set-up for solid powder aluminizing was established. The first aluminizing experiment was successfully performed and the C45 steel substrate was coated with a uniform FeAl layer. This experimental work gives the basis of the research, in which the next step is to

examine the wetting conditions between aluminized steel specimens and lead-free solder melts, and the behaviour of the aluminized specimens against lead-free solder melts for prolonged durations.

Acknowledgments

The authors are grateful for Anikó Márkusné and Sándor Boda for establishing the aluminizing container and the sample preparations.

References

[1] Kim K. S., Huh S. H., and Suganuma K. (2003). Effects of intermetallic compounds on properties of Sn-Ag-Cu lead-free soldered joints, Journal of Alloys and Compounds. 352, no. 1-2, 226–236, **https://doi.org/10.1016/S0925-8388(02)01166-0**

[2] Wu C. M. L., Yu D. Q., Law C. M. T., and Wang L., (2004). Properties of lead-free solder alloys with rare earth element additions, Materials Science and Engineering R. 44, no. 1,1–44, 2-s2.0-1642324965, **https://doi.org/10.1016/j.mser.2004.01.001**

[3] Farooq, M., Ray S., Sarkhel A., and Goldsmith C. (2001). Evaluation of lead(Pb)-free ceramic ball grid array (CBGA): wettability, microstructure and reliability, 51st Electronic Components and Technology Conference, June usa, 978–986, **https://doi.org/10.1109/ECTC.2001.927927**

[4] Yoon, J.-W., Kim S.-W., and Jung S.-B., (2005). IMC morphology, interfacial reaction and joint reliability of Pb-free Sn-Ag-Cu solder on electrolytic Ni BGA substrate, Journal of Alloys and Compounds. (392, no. 1-2, 247–252, **https://doi.org/10.1016/j.jallcom.2004.09.045**

[5] Yu D. Q. and Wang L., (2008). The growth and roughness evolution of intermetallic compounds of Sn-Ag-Cu/Cu interface during soldering reaction, Journal of Alloys and Compounds. 458, no. 1-2, 542–547, **https://doi.org/10.1016/j.jallcom.2007.04.047**

[6] Kondo, M., Ishii, M., Muroga, T. (2015). Corrosion of steels in molten gallium (Ga), tin (Sn) and tin lithium alloy (Sn–20Li). Fusion Eng. Des., 98–99, 2003–2008. **https://doi.org/10.1016/j.fusengdes.2015.05.051**

[7] Heinzel, A., Weisenburger, A., Müller, G. (2017). Corrosion behavior of austenitic steel AISI 316L in liquid tin in the temperature range between 280 and 700 °C. Mater. and Corr., 68 (8), 831–837. **https://doi.org/10.1002/maco.201609211**

[8] Kang S. K., Leonard D., Shih D. A. Y., Gignac L., Henderson D. W., Cho S., and Yu J. (2006). Interfacial reactions of Sn-Ag-Cu solders modified by minor Zn alloying addition, Journal of Electronic Materials. 35, no. 3, 479–485, 2-s2.0-33645566980, **https://doi.org/10.1007/BF02690535**

[9] Nishikawa, H., Komatsu, A., Takemoto, T. (2005). Interfacial reaction between Sn–Ag–Co solder and metals. Materials Transactions, 46 (11), 2394–2399. Special Issue on Lead-Free Soldering in Electronics III 2005 The Japan Institute of Metals. **https://doi.org/10.2320/matertrans.46.2394**

[10] Watanabe, J., Hatsuzawa, K., Ogata, S., Yoshida, S., Shohji, I. (2019). Erosion resistance properties of iron–carbon composite plating to molten lead-free solder. Appl. Sci., 9 (13), 2724. **https://doi.org/10.3390/app9132724**

[11] Benke, M., Salyi, Z., Takats, V., Csik, A., Rugoczky, P., Kaptay, G. (2019). The behavior of steel coated with TiB_2 in Sn-Ag-Cu melt. Materials Science and Technology, 35 (6), 680–686. **https://doi.org/10.1080/02670836.2019.1582192**

[12] Salyi, Z., Kaptay, G., Koncz-Horvath, D., Somlyai-Sipos, L., Kovacs, P. Z., Lukacs, A., Benke, M. (2022). Boride coatings on steel protecting it against corrosion by a liquid lead-free solder

alloy. Metall. Mater. Trans. B, 53, 730–743. **https://doi.org/10.1007/s11663-021-02412-2**
[13] Bayer, G. (1995). Vapor aluminum diffused steels for high-temperature corrosion resistance. Materials Performance, 34, 34–38.
[14] Bates, B., Wang, Y., Zhang, Y. (2009). Formation and oxidation performance of low-temperature pack aluminide coatings on ferritic–martensitic steels. Surface and Coatings Technology, 204 (6–7), 766–770. **https://doi.org/10.1016/j.surfcoat.2009.09.063**
[15] Yao Teng Steel Brand. **https://www.astmsteel.com/product/c45-round-bar-aisi-1045-din-jis-s45c/**
[16] Metal Powder Company Limited (MEPCO). **https://www.mepco.co.in/about-us**
[17] PGchem company. **https://www.pgchem.sk/en/terms-and-conditions**
[18] White Falcon Dental. **https://wfdental.hu/**
[19] Muhelynet. **https://muhelynet.hu/**